HIGH IMPEDANCE FAULT DETECTION

F. B. Costa[1*], G. R. S. Lira[2], W. C. Santos[2], J. A. C. B. Silva[2], B. A. Souza[2], N. S. D. Brito[2], M. R. C. Paes Jr[3]
[1]Federal University of Rio Grande do Norte, Campus Univesitário Lagoa Nova, Natal - RN, Brazil.
[2]Federal University of Campina Grande, 882 Aprígio Veloso Av, Bodocongó, Campina Grande - PB, Brazil.
[3]Energisa, BR 230, km 25 - Cristo Redentor, 58.071-680, João Pessoa - PB, Brazil.
*E-mail: flabc@ee.ufcg.edu.br.

Abstract: This paper presents the analysis of actual oscillographic records with high impedance faults (HIFs) upon various contact surfaces in order to identify the main characteristics of such fault in both time and wavelet domains. The features of HIFs extracted by means of the wavelet coefficient energies of the maximal overlap discrete wavelet transform (MODWT) have been used for developing a new detection method to yield results in satisfactory agreement with real applications. The proposed HIF detection method was installed at a local utility substation and good results have been obtained.

1. INTRODUCTION

High impedance faults (HIFs) result when an energized conductor of the primary network makes unwanted electrical contact with a road surface, a sidewalk surface, a tree limb, or some other surface with high resistive value which restricts the flow of fault current to a level below that detectable by conventional protective devices. Therefore, the energized conductor on the ground surface poses a danger to the public. In addition, the arcing poses a fire hazard.

Once the conventional protective devices can not properly detect HIFs, the post-analysis of actual records with HIFs has become an important issue to find HIF characteristics in voltage and current waveforms that would make detection possible and practical to ensure the safety of power system equipment as well as the general public.

It is well known that HIF currents present typical characteristics such as buildup, shoulder, nonlinearity, asymmetry, intermittence, and high frequency transients [1, 2]. Once voltages and currents in HIFs are non-stationary signals in time and frequency domains, these signals can be properly analyzed by using the wavelet transform. Much research has been focused on wavelet-based techniques applied on analyzing power system transients [3], detecting and classifying power quality disturbances [4, 5] and faults [6, 7]. Wavelet-based detection methods of distribution HIFs have also been proposed [2, 8, 9]. Beyond the wavelet transform, many techniques have been proposed to improve the detection of HIFs [10].

The aim of this paper is to analyze actual oscillographic records with HIFs upon various contact surfaces in order to identify the main characteristics of this fault in both time and wavelet domains. HIFs have been assessed with actual oscillographic records measured by digital fault records (DFRs) from a Brazilian Power System Utility.

This paper presents also a wavelet-based method as a fast and efficient tool to extract information regarding the HIFs. The features of HIFs extracted by means of the wavelet coefficient energies of the maximal overlap discrete wavelet transform (MODWT) have been used for developing a new detection method to yield results in satisfactory agreement with real applications. The proposed HIF detection method was installed at a substation and good results have been obtained.

2. WAVELET COEFFICIENT ENERGIES

The wavelet transform is a well-known powerful tool to analyze a signal within different frequency ranges by dilating and translating the mother wavelet. Besides the discrete wavelet transform (DWT), the MODWT uses also low- and high-pass filters (scale and wavelet filters) to divide the frequency-band of the input signal into low- and high-frequency components (approximation and wavelet coefficients). This operation may be repeated recursively, feeding the low-pass filter output into another identical filter pair, decomposing the signal into approximation (a) and wavelet (w) coefficients at various scales. However, in contrast to the DWT, there is no down-sampling in MODWT (time-invariant transformation) [11]. In this way, the transients in faults can be faster detected by means of the MODWT [12]. In this paper, both the approximation and wavelet coefficients are computed through the MODWT.

The coefficients of the filter pairs are associated with the selected mother wavelet. The wavelet Daubechies 4 (db4) was used in this paper due to its good time resolution that provides an accurate identification of fast transients [7, 13].

According to [2], HIFs generate high frequency components between 2 and 10 kHz. In this paper, the voltages and currents with HIFs were gathered from DFRs with sampling rate of f_s=15360 Hz. From the Nyquist theorem, a discrete signal with sampling rate of f_s has frequency components limited from 0 to $f_s/2$. In addition, the process to computer the approximation and wavelet coefficients divides the frequency spectrum of the original signal into octave bands [11]. Therefore, the frequency spectrum of the wavelet coefficients at the first scales are related to the highest frequency components of the signal and can be used to detect transient generated by HIFs. In this paper, the wavelet coefficients at the first three scales are used by proposed method in order to detect the high frequency components of the transients in HIFs.

In order to compute the energies of the wavelet coefficients, at scale j, a sliding data window goes through w_j, shifting one coefficient at a time, viz

$$\mathcal{E}_j(k) = \begin{cases} \sum_{n=1}^{\Delta k} w_j^2(n), & \text{if} \quad 1 \leqslant k \leqslant \Delta k \\ \sum_{n=k-\Delta k+1}^{k} w_j^2(n), & \text{if} \quad \Delta k < k \leqslant k_t \end{cases} \tag{1}$$

where: Δk is the window length, $k = \{1, 2, \ldots, k_t\}$, j=$\{1, 2, 3\}$, and k_t is the total number of samples of the input signal. In this paper, Δk== f_s/f is the amount of samples contained in one cycle of the fundamental power frequency, where f_s is the sampling rate and f is the fundamental power frequency.

3. MAIN FEATURES OF HIF

The main characteristics of HIFs are the low fault current magnitude and the arcing current. A HIF presents a typical current of 10-50 A [14]. As a consequence, HIFs cannot be easily detected or cleared by conventional protective devices due to theirs low fault current magnitudes [15].

Arcing is the result of the air gaps due to the poor contact made with the ground. These air gaps create a high potencial over a short distance and arcing is produced from the air gap breaking down. However, the arc current in HIFs is small and its arc length is short compared to that arcs under other conditions. For instance, the sustained arc in faults upon transmission circuits can elongate to many feet and the initial arc current of thousands of amperes can vaporize the conductor causing metallic ions to contribute to a low arc resistance. On the other hand, HIFs may involve an arc length of few inch and the initial current may be less than a hundred amperes [16]. Figure 1 depicts an actual oscillographic record regarding an HIF on dry sand. In this case, the maximum current magnitude reaches about 30 A.

HIF currents present typical characteristics, summarized as follows [1]:

- Buildup: ground fault current grows to its maximum value in about tens of cycles.
- Shoulder: buildup is ceased for few cycles.
- Nonlinearity: the voltage-current characteristic curve of HIF is nonlinear.
- Asymmetry: fault current has different waveforms for positive and negative half cycle.
- Intermittence: the energized wire interrupts the contact with the soil at some cycles. The arcing can be reduced hardly and restored back.

One of the main HIF characteristics is the buildup effect: the current grows to its maximum value in about tens of cycles. According to [16], the reduced initial current is due to a smaller effective initial contact between the conductor and the soil. When the contact area is small, the density of the current at arc/soil interface is large. This will result in localized arcing and ionization. The arc will then penetrate the ground between the soil particles, enlarging the effective contact with the ground. Figure 1 shows the buildup effect at the beginning of the HIF.

When the current is growing to its maximum value the buildup can cease for a while. This characteristic is known as shoulder [1]. According to Figure 1, the initial fault current took about 10 cycles to reach its maximum value. However, the buildup is ceased for 3 cycles around the 5th cycle after the beginning of the HIF.

The mechanism of arc formation is a predominant factor in the non-linearity of the fault impedance. According to [16], an arc forms when the voltage is sufficient to break down small air gaps between the conductor and earth. The arc strikes and extinguishes every half-cycle and the arc current flows during a portion of the cycle. As a consequence, the current waveform present distortions, having pronounced peaks and short periods during which the current remains flat at zero (Figure 1).

Distorted arc currents in HIF are rich in harmonic and non-harmonic components. The magnitude of the resulting harmonic currents appear sufficiently predictable to be utilized in HIF detectors [16]. In addition, a typical current with HIF is also characterized by high frequency transients [2].

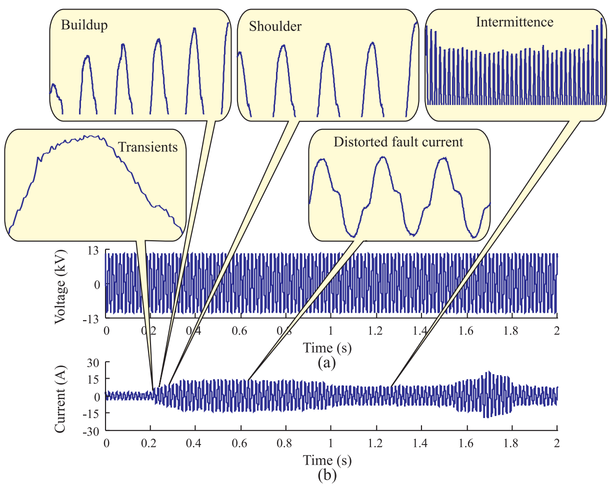

Figure 1: Actual oscillographic record with HIF on wet pavement: (a) voltage; (b) current.

4. ANALYSIS OF ACTUAL HIF CURRENTS

In order to collect HIF data to access the features of these faults and assist the development of a HIF detector, staged fault tests were performed on a distribution feeder in Boa Vista town, Brazil, whose main features were:

- HIF tests were done on six different kinds of contact surfaces: grass, crushed stone, pavement, asphalt, sand, and local soil.
- All HIFs were staged on dry and wet surfaces.
- A two-meter pole was placed between the common pole and the HIF point, where potential and current transformers were installed.
- A 13.8 kV conductor coming from the common pole was connected to the transition pole and to an insulating rod.
- An insulating scaffold was placed in order to enable security for the responsible technician.
- Isolation and signalizing of the testing area were properly accomplished.
- A local fuse link was used to control the current magnitude during the staged faults.
- A 15360 Hz sampling frequency DFR was installed at the fault point in order to enable the measurement, recording, and viewing of the events to be generated in the tests. All records were recorded with length of 30 s.
- Other DFRs were installed far 1 and 11 km from the fault point.

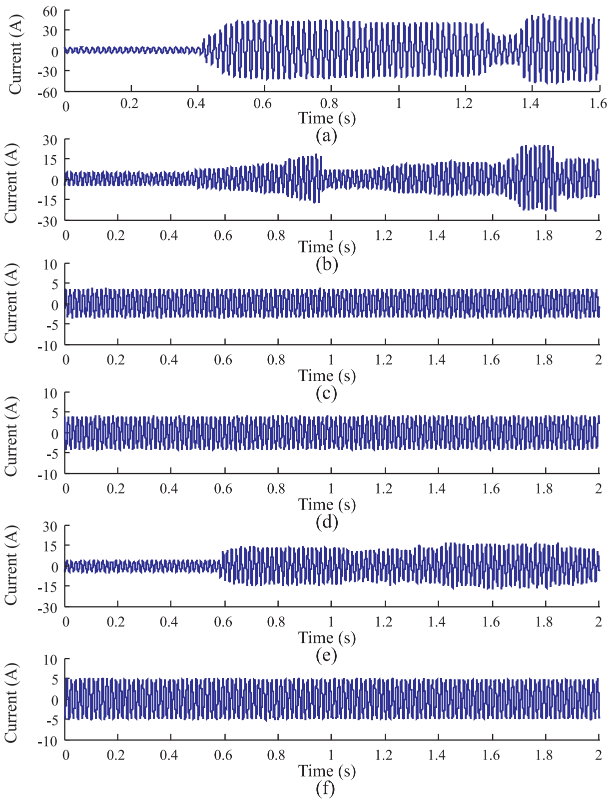

Figure 2: Actual currents with HIF on dry surfaces: (a) grass; (b) pavement; (c) crushed stone; (d) asphalt; (e) sand; (f) local soil.

Figure 2 depicts fault currents with HIF on dry surfaces: grass, pavement, crushed stone, asphalt, sand, and local soil, respectively. These currents were measured far 11 km from the fault point. As expected, the HIF features changed with the contact surface of the fault. The HIF was more severe on grass surface where the current reached a maximum value of about 60 A. HIFs on dry grass, pavement, crushed stone, and sand presented one or more of the HIF characteristics addressed before, such as buildup and shoulder. On the other hand, HIFs on both dry asphalt and local soil did not involve an arc at the point of contact with dry surfaces. As a consequence, the fault current did not present typical HIF features.

It is well known that currents during HIFs are nonstationary in both time and frequency domains when there is an arc formation at the point of contact. As a consequence, such signals can be properly analyzed by using the MODWT.

Figure 3 depicts the normalized wavelet coefficient energies, at first scale, of the fault currents shown in Figure 2. The energies in all records were normalized with base energies obtained during the steady-state system operation (before the HIF). Reference lines (red dot lines) twice the base energies were plotted in order to identify changes in energies during the HIF.

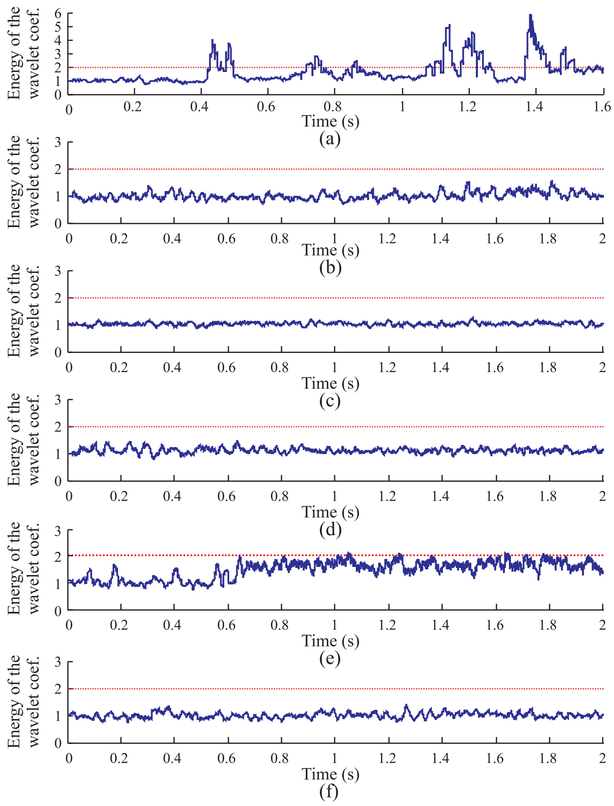

Figure 3: Wavelet coefficient energies of HIF currents on dry surfaces: (a) grass; (b) pavement; (c) crushed stone; (d) asphalt; (e) sand; (f) local soil.

According to Figure 3, the wavelet coefficient energies related to the steady-state system operation (due to electrical noises) presented values almost constant. However, during the fault, the wavelet coefficient energies in HIFs on dry grass and sand presented features different from the steady-state interval (increasing of energy). Such energy features can be used to detect some types of HIFs on dry surfaces. However, the wavelet coefficient energies, at first scale, of the currents in HIFs on dry pavements, crushed stone, asphalts, and local soils did not present a signature to be used for HIF detection.

No matter what method is used, not all HIFs are detectable [14]. It is difficult for any HIF detector to sense the fault when the conductor near the end of the feeder breaks and falls on a surface such as the asphalt and the arc current is not formatted.

As expected, after the analysis of the records with HIF on different fault surfaces, it was observed that the features of HIFs change with the contact surface. Beyond the contact surface, the weather is another factor which may influence HIF characteristics. In this paper, all HIFs were staged on both dry and wet surfaces. Figure 4 depicts fault currents, at phase A, with HIF on wet surfaces: grass, pavement, crushed stone, asphalt, sand, and local soil, respectively. These currents were measured far 11 km from the fault point.

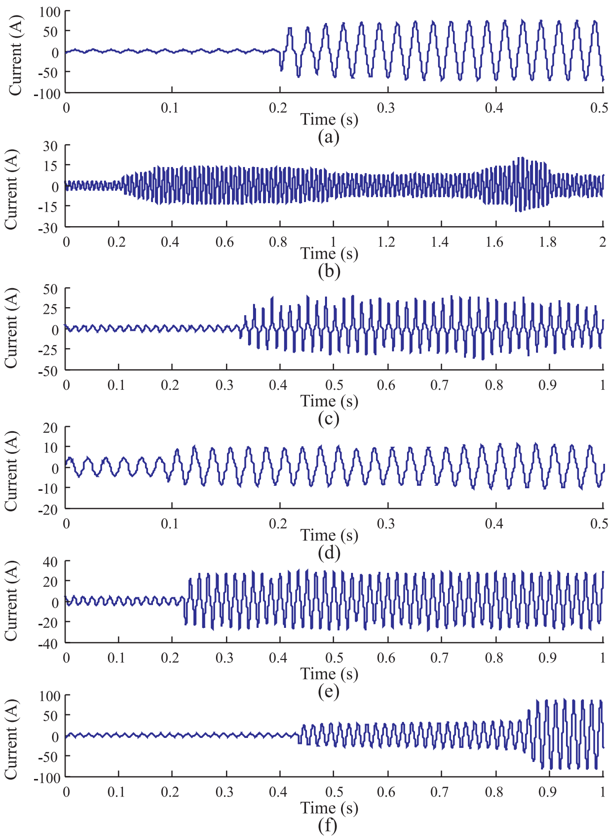

Figure 4: Actual current with HIF on wet surfaces: (a) grass; (b) pavement; (c) crushed stone; (d) asphalt; (e) sand; (f) local soil.

The analysis of the staged HIFs states that the arc was formatted on all wet surfaces. In all these cases, the fault currents presented typical features of HIFs. In addition, the HIF current was more severe on wet surface instead the dry one.

Figure 5 depicts the normalized wavelet coefficient energies, at first scale, of the fault currents shown in Figure 4. The energies in all records were normalized with base energies obtained during the steady-state system operation (before the HIF).

According to Figure 5, the wavelet coefficient energies related to the steady-state system operation presented values almost constant. However, during the fault, the energies due to HIFs on wet grass, crushed stone, sand, and local soil increased above the reference energy. On the other hand, the wavelet coefficient energies related to HIFs on wet pavement and asphalt did not present a significant signature to be used for HIF detection.

According to Figures 2(e) and 3(e), the current of the HIF on dry sand surface could not be properly detected by means of the wavelet coefficient energy analysis at the first scale. The feature extraction in HIFs on some contact surfaces such as pavement and asphalt is not so easy at the first scale and the analysis of the wavelet coefficient energies at more wavelet scales is required.

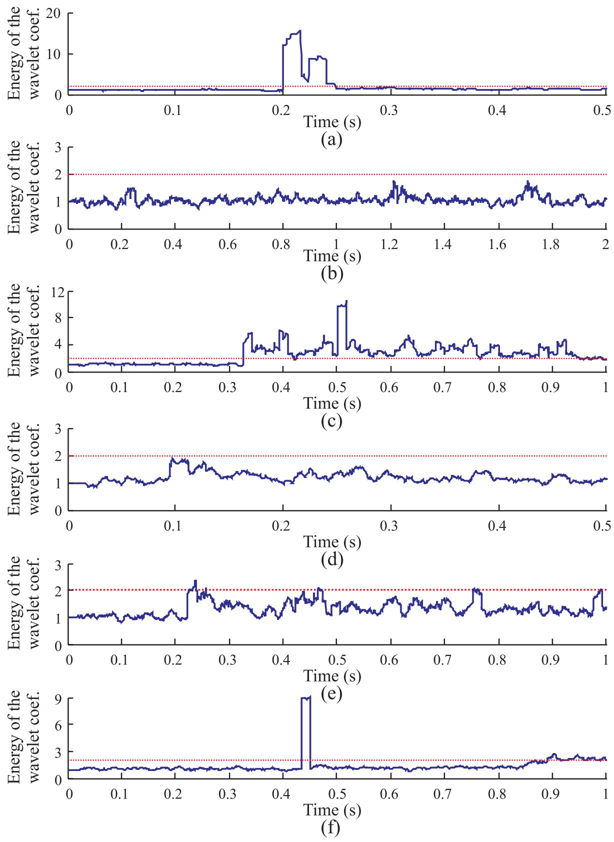

Figure 5: Wavelet coefficient energies of HIF currents on wet surfaces: (a) grass; (b) pavement; (c) crushed stone; (d) asphalt; (e) sand; (f) local soil.

Figure 6 depicts the current of a HIF on dry sand surface (Figs. 2(d)) and the respective wavelet coefficient energies at the first three scales. In this case, the HIF features could be detected at the last two scales.

Typically, a stable arc current is not immediately formed on some kind of contact surfaces, specially in dry surfaces, but several strikes (sparks) occur within a short period of time until a stable arc is established [17]. According to Figure 6, several sparks could be detected before the arc formation through the analysis of the wavelet coefficient energies at the last two scales, as well as the HIF.

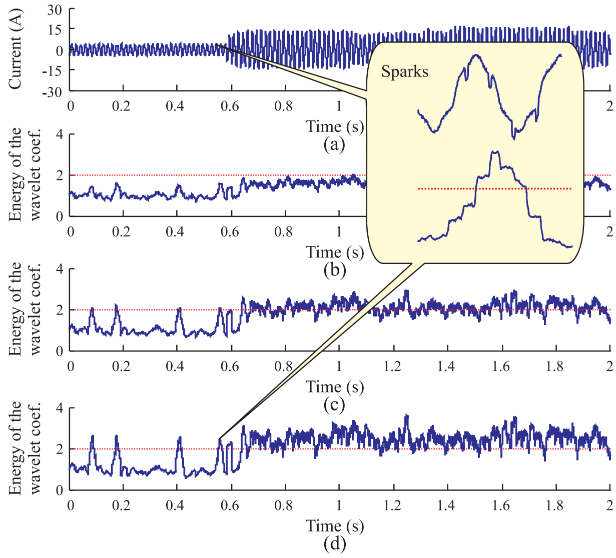

Figure 6: Actual HIF on dry sand surface: (a) fault current; (b) wavelet coefficient energies at first scale; (c) wavelet coefficient energies at second scale; (d) wavelet coefficient energies at third scale.

4.1. WAVELET-BASED HIF DETECTION

Figure 7 depicts the simplified flowchart of the proposed method. At first, three stages of the MODWT with db4 is applied in all phase currents followed by the wavelet coefficient energy computation in such scales. These energies are evaluated by the HIF detection block in order to detect the fault.

Adaptive thresholds for each wavelet coefficient energy in all evaluated scales are computed as twice of the average energy in one second during the steady-state operation. A HIF is detected when at least one of the wavelet coefficient energy waveform presents magnitude higher than the respective threshold for several cycles (Figures 3, 5, and 6)

Table 1 summarizes the performance of the proposed MODWT-based detection method in various staged HIFs. The detection of the HIF upon wet surfaces presented better performance than such fault upon dry surfaces. With regard to the dry surfaces, almost all the HIFs on crushed stones and asphalt could not be detected.

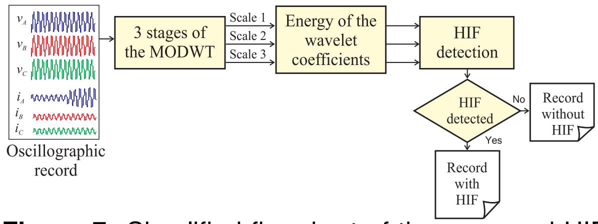

Figure 7: Simplified flowchart of the proposed HIF detection method.

The wavelet coefficient energy analysis of the currents can be used for transient detection of HIFs on most contact surfaces. However, these energy waveforms can also be used to discriminate HIF from other disturbances such as faults and power quality disturbances [5, 18, 19]. Some signatures to distinguish HIFs from other disturbances with transients are described as follows:

- Faults upon transmission and distribution systems are usually characterized by voltage sags during the fault-clearing time. Some power system operations, such as a heavy load switching are also characterized by voltage sags. On the other hand, a typical HIF does not generate voltage sags at substation.
- A typical fault on overhead transmission and distribution lines is cleared by protection system or protection equipment as soon as possible. As a consequence, the wavelet coefficient energies present high values during few cycles. On the other hand, a typical HIF presents low current magnitude and the fault is not cleared by conventional protection relaying. As a consequence, the wavelet coefficient energies may present high values for a long time.
- The switching operation to energize/deenergize lines, power capacitor banks, and other equipment is also transient in nature. However, in contrast to HIF, the transients are damped in few cycles after the switching (the wavelet coefficient energies present high values during few cycles after the switching).
- Faults and transients due to switching operation present high value of wavelet coefficient energies of both voltages and currents during the event (hundreds or thousands of the reference energy), specially at the beginning time, whereas the wavelet coefficient energies of the fault current in HIF may present a small increasing.

Table 1: Performance evaluation of the MODWT-based method far 11 km from the staged HIF.

Contact surface of the HIF	Amount of records dry	Amount of records wet	HIF detected dry	HIF detected wet
Grass	5	5	5	5
Pavement	5	8	4	6
Crushed stone	5	5	0	5
Asphalt	5	7	1	6
Sand	6	4	3	4
Local soil	9	6	7	5

Nowadays, the proposed MODWT-based detection method is installed in a feeder belongs a Brazilian Utility to analyze oscillographic data from a specific DFR, which was set to record oscillographic data every 30 s. Each record has length of 30 s. The main goal is to develop the HIF discrimination step in which a HIF will be properly distinguished from other faults and power quality disturbances.

After the implementation of the HIF discrimination method the proposed method will be implemented into a DSP (Digital Signal Processing) in order to detect HIF in real-time.

5. CONCLUSIONS

The wavelet coefficient energies as a fast and efficient tool in analyzing high impedance faults was presented in this paper. The performance of the method was evaluated with actual records obtained far 11 km from staged high impedance faults upon various dry and wet contact surfaces. With exception of the dry crushed stones and dry asphalts, good results were obtained.

Analysis of actual oscillographic data has been reveled some features of high impedance faults which are unusual in simulation. Therefore, the performance evaluation of a method with actual data taking into account different high impedance faults is important in the context of practical applications.

The proposed method will be further implemented to detect high impedance faults in real-time.

REFERENCES

[1] S. R. Nam, J. K. Park, Y. C. Kang, and T. H. Kim. A modeling method of a high impedance fault in a distribution system using two series time-varying resistances in EMTP. *IEEE Transactions on Power Delivery*, vol. 3, pp. 1175–1180, 2001.

[2] A.-R. Sedighi, M.-R. Haghifam, O. Malik, and M.-H. Ghassemian. High impedance fault detection based on wavelet transform and statistical pattern recognition. *IEEE Trans. on Power Delivery*, vol. 20, no. 4, pp. 2414 – 2421, 2005.

[3] F. B. Costa, B. A. Souza, and N. S. D. Brito. A wavelet-based algorithm to analyze oscillographic data with single and multiple disturbances. *IEEE PES General Meeting*, Pittsburgh, USA, jun 2008.

[4] O. Poisson, P. Rioual, and M. Meunier. Detection and Measurement of Power Quality Disturbances Using Wavelet Transform. *International Conf. on Harmonics and Quality of Power*, pp. 1125–1130, Athens, Greece, Oct. 1998.

[5] F. B. Costa, B. A. Souza, and N. S. D. Brito. Detection and Classification of Transient Disturbances in Power Systems. *IEEJ Trans. PE*, pp. 910–916, Oct 2010.

[6] O. A. S. Youssef. Fault classification based on wavelet transforms. *Transmission and Distribution Conference and Exposition*, vol. 1, pp. 531–536, Nov 2001.

[7] K. M. Silva, B. A. Souza, and N. S. D. Brito. Fault Detection and Classification in Transmission Lines Based on Wavelet Transform and ANN. *IEEE Transactions on Power Delivery*, vol. 21, no. 4, pp. 2058–2063, Oct 2006.

[8] D. C. T. Wai and X. Yibin. A novel technique for high impedance fault identification. *Power Delivery, IEEE Transactions on*, vol. 13, no. 3, pp. 738 –744, Jul. 1998.

[9] T. Lai, L. Snider, E. Lo, and D. Sutanto. High-impedance fault detection using discrete wavelet transform and frequency range and RMS conversion. *IEEE Trans. on Power Delivery*, vol. 20, no. 1, pp. 397 – 407, Jan. 2005.

[10] L. Li and M. Redfern. A review of techniques to detect downed conductors in overhead distribution systems. In *Seventh International Conference on Developments in Power System Protection (IEE)*, pp. 169 –172. 2001.

[11] D. B. Percival and A. T. Walden. *Wevelet Methods for Time Series Analysis*. New York, USA: Cambridge University Press., 2000.

[12] F. B. Costa, B. A. Souza, and N. S. D. Brito. Real-time detection of fault-induced transients in transmission lines. *IET Electronics Letters*, pp. 753–755, May 2010.

[13] M. H. J. Bollen and I. Y.-H. Gu. *Signal Processing of Power Quality Disturbances*. New York, USA: Wiley-IEEE Press, 2006.

[14] B. Aucoin and R. Jones. High impedance fault detection implementation issues. *IEEE Transactions on Power Delivery*, vol. 11, no. 1, pp. 139 –148, jan 1996.

[15] R. NAKAGOMI. *Proposição de um sistema para simulação de faltas de alta impedância em redes dedistribuição*. Ph.D. thesis, University of São Paulo, São Paulo, Brazil, 2006.

[16] D. I. Jeerings and J. R. Linders. Ground Resistance - Revisited. *IEEE Transactions on Power Delivery*, vol. 4, no. 2, pp. 949–956, April 1989.

[17] B. M. Aucoin and B. D. Russell. Distribution High Impedance Fault Detection Utilizing High Frequency Current Components. *Power Engineering Review, IEEE*, vol. PER-2, no. 6, pp. 46 –47, june 1982.

[18] F. B. Costa. *Uma Técnica de Diagnóstico em Tempo Real de Distúrbios Transitórios Baseada na Transformada Wavelet Para Uso em Registradores Digitais de Perturbação*. Ph.D. thesis, Federal University of Campina Grande, Campina Grande, Brazil, 2010.

[19] F. B. Costa, B. A. Souza, and N. S. D. Brito. Discrete Wavelet Transform in Power Systems: Transient Disturbance Analysis. *International Symposium on High Voltage Engineering*, Cape Town, South Afric, Aug 2009.